UNIVERSITI TEKNOLOGI MALAYSIA
www.utm.my

Bengkel Penerbitan Monograf

19 Mac 2014

Rosli Hussin

Pengerusi Panel Buku Penyelidikan/Book Chapter
Penerbit UTM Press
Universiti Teknologi Malaysia,
Johor

5

CopyWrite Issue

Policy on Academic Integrity

"Plagiarism is the intentional or unintentional representation of another person's idea or product as one's own. Plagiarism includes, but is not limited to, the following: copying verbatim all or part of another's written work or using phrases, charts, figures, illustrations or mathematical or scientific solutions without citing the source; paraphrasing ideas, conclusions or research without citing the source, and using all or part of a literary plot, poem, film, musical score or other artistic product without attributing the work or its creator. Writer/editor can avoid unintentional plagiarism by carefully following accepted scholarly practices. Notes taken should accurately record sources of material to be cited, quoted, paraphrased or summarized, and the monograph/Book should acknowledge these sources in footnotes and/or endnotes

Sketch & Schematic

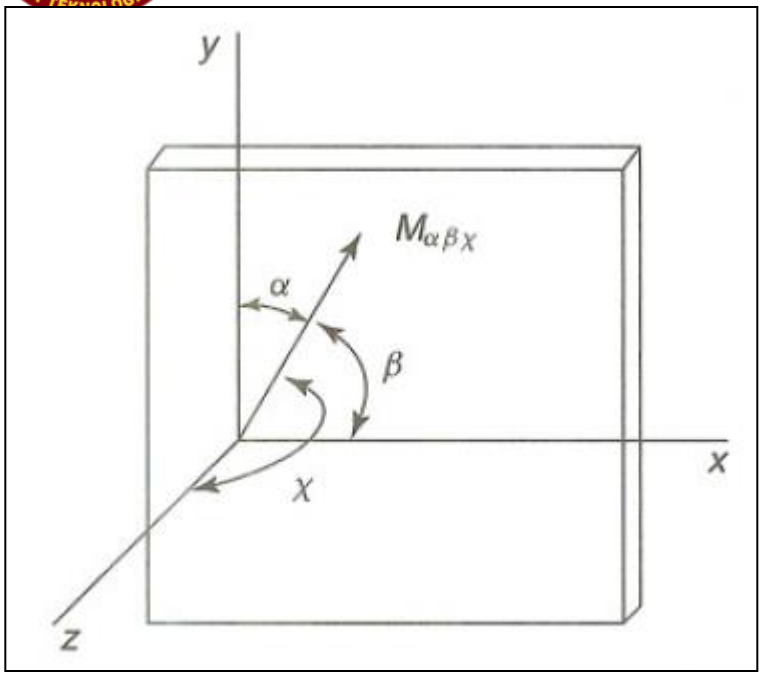

Figure 1. Location of sample in a Cartesian coordinate system. [Reproduced with permission from Fina and Koenig,[6] Figure 1. Copyright 1986 John Wiley & Sons.]

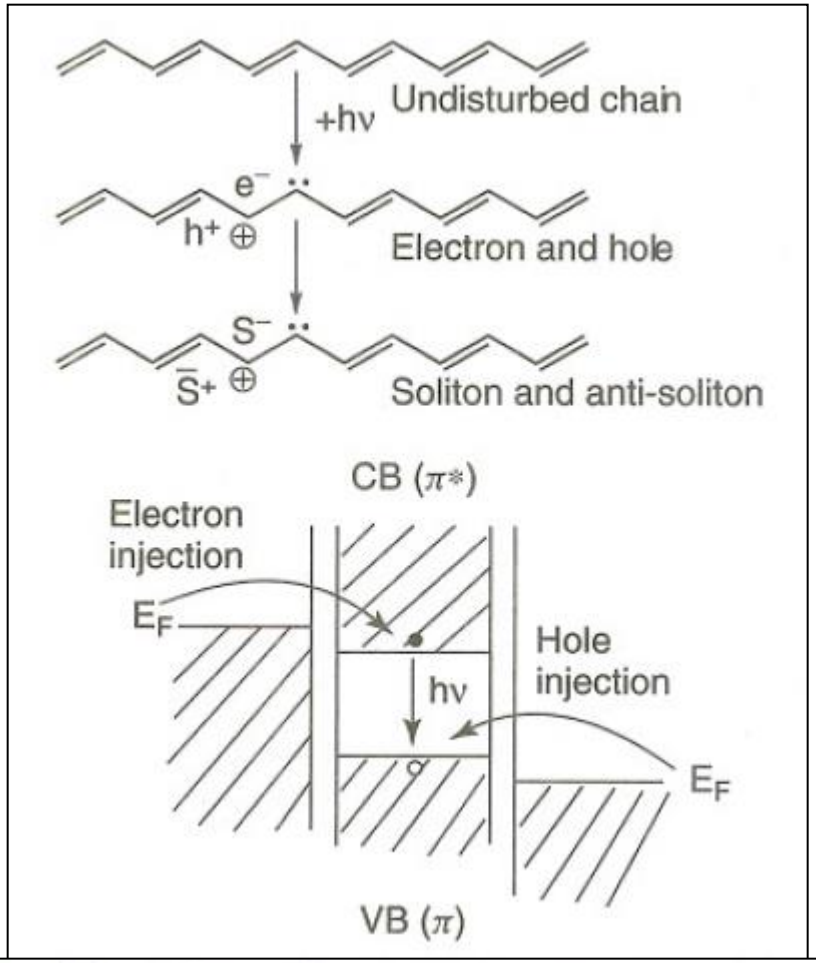

Figure 24. Scheme for the photogeneration of charged carriers in polyconjugated systems. [Reproduced from Blanchet *et al.*[122], p 99.]

Sketch & Schematic

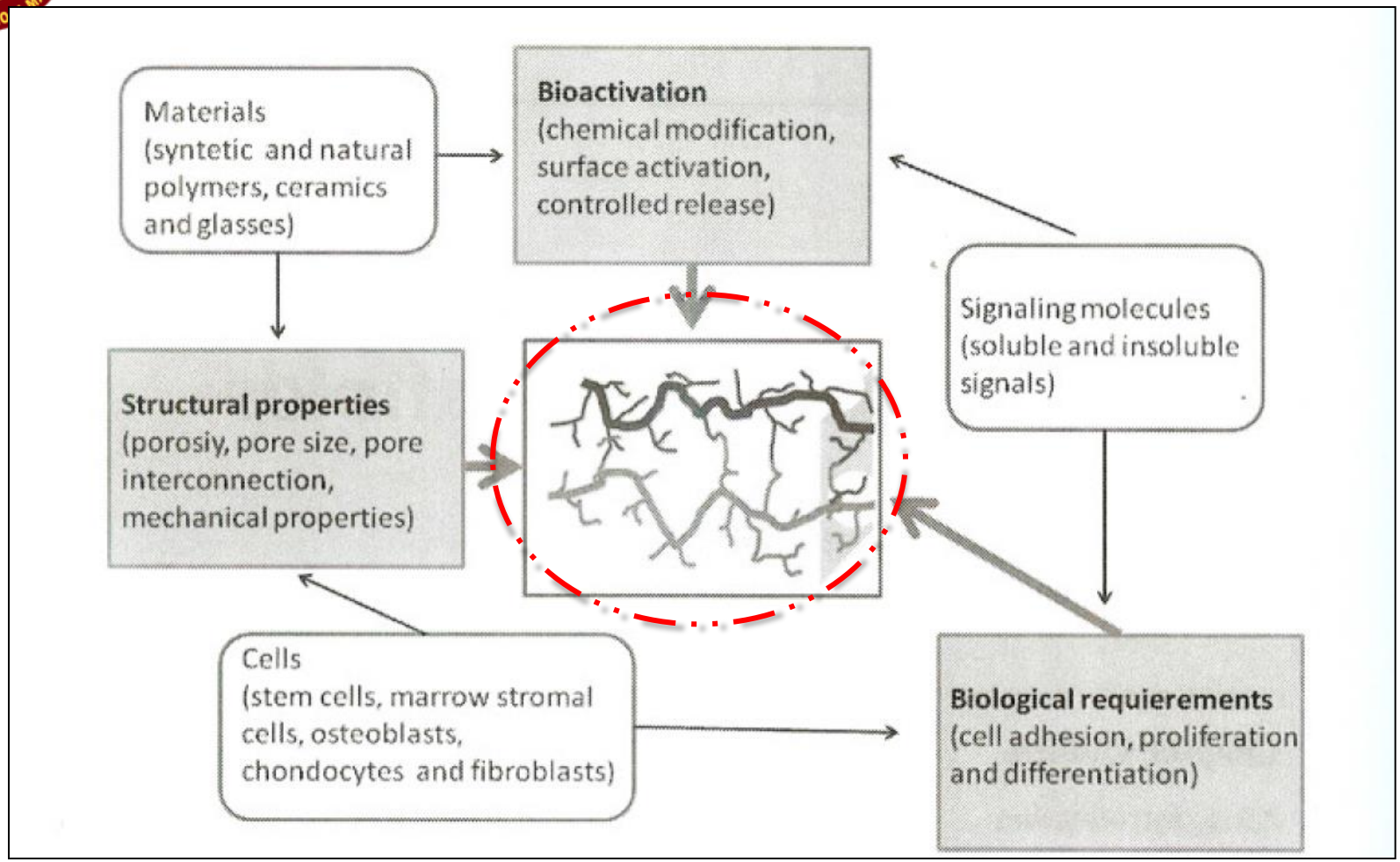

FIGURE 7.1.1 Schematic diagram of key factors involved in the design of optimal scaffolds for bone tissue engineering. *Modified after Ref. [1].*

Sketch & Schematic

Polarizer Design

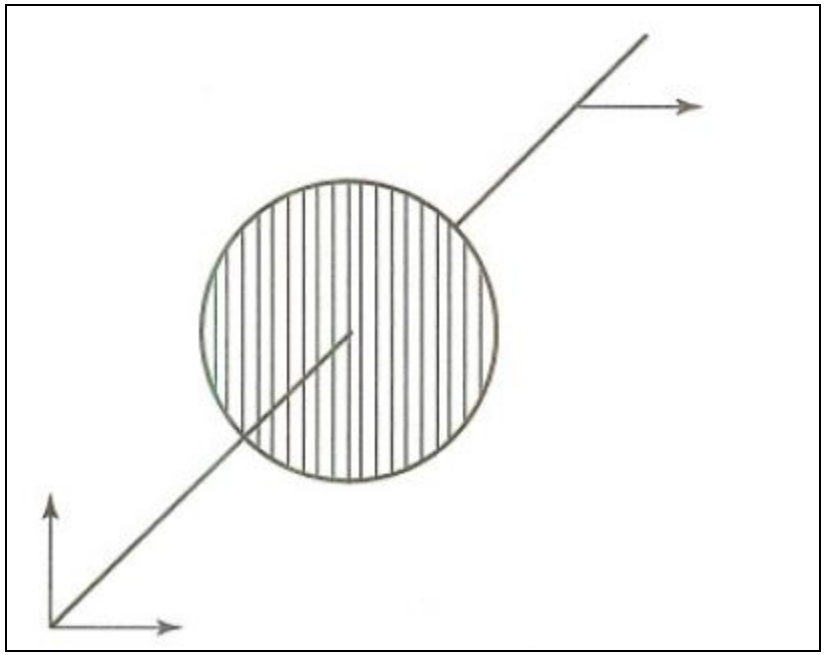

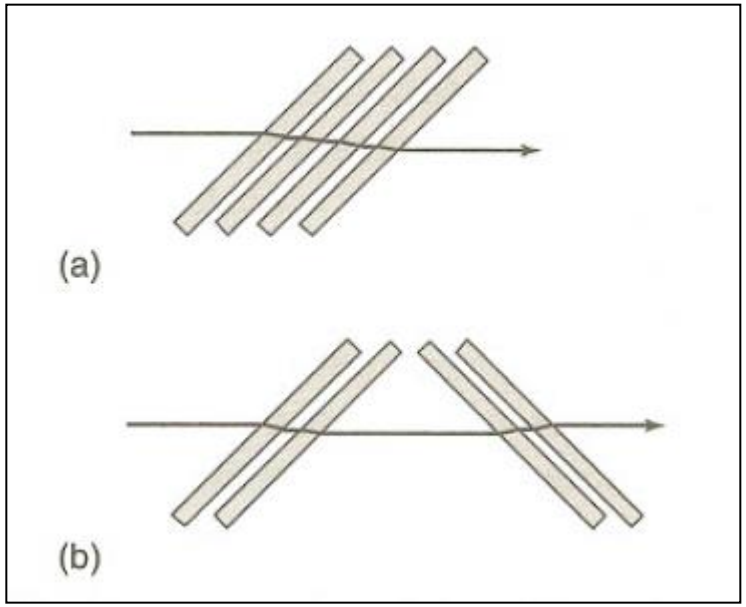

Figure 2. Brewster angle polarizer. [Reproduced from Thierry Buffeteau and Michel Pézolet, 'Linear Dichroism in Infrared Spectroscopy', in "Handbook of Vibrational Spectroscopy", eds J.M. Chalmers and P.R. Griffiths, John Wiley & Sons, Chichester, 693–710, Vol. 1 (2002).]

Figure 1. Wire-grid polarizer. [Reproduced from Thierry Buffeteau and Michel Pézolet, 'Linear Dichroism in Infrared Spectroscopy', in "Handbook of Vibrational Spectroscopy", eds J.M. Chalmers and P.R. Griffiths, John Wiley & Sons, Chichester, 693–710, Vol. 1 (2002).]

Sketch & Schematic

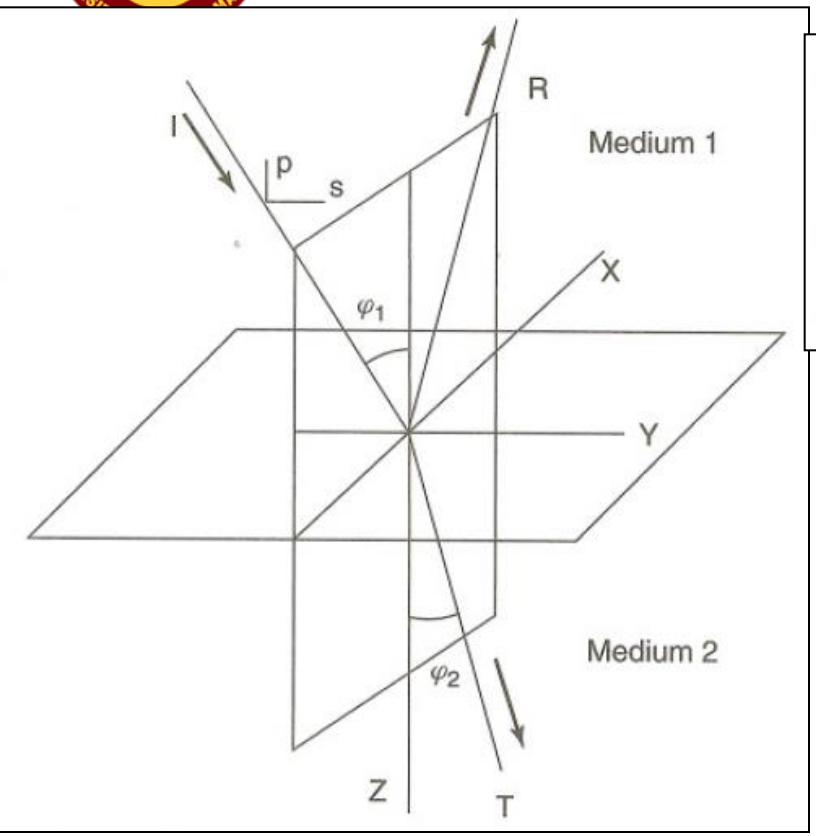

Figure 2. Geometry of reflection (R) and transmission (T) at an interface in the X, Y plane of an incident ray I. [Adapted from G.H. Meeten, in 'Optical Properties of Polymers', G.H. Meeten, ed, Elsevier Applied Science, London, 54–58 (1986), with kind permission from Kluwer Academic Publishers.[2]]

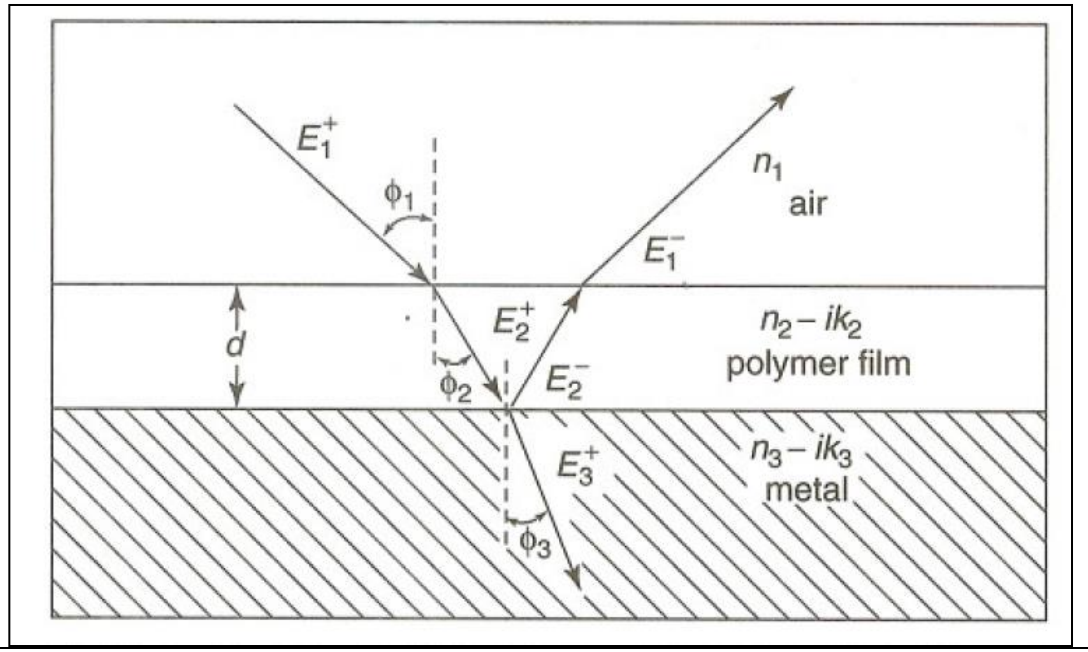

Figure 3. Ray diagram of the IR-RA experiment for a polymer-coated metal. The subscripts 1, 2 and 3 on the optical constants correspond to the electromagnetic wave in air, polymer film, and metal, respectively. [Adapted from Greenler[32] with permission from the American Institute of Physics.]

Layout (Diagram) Instrument

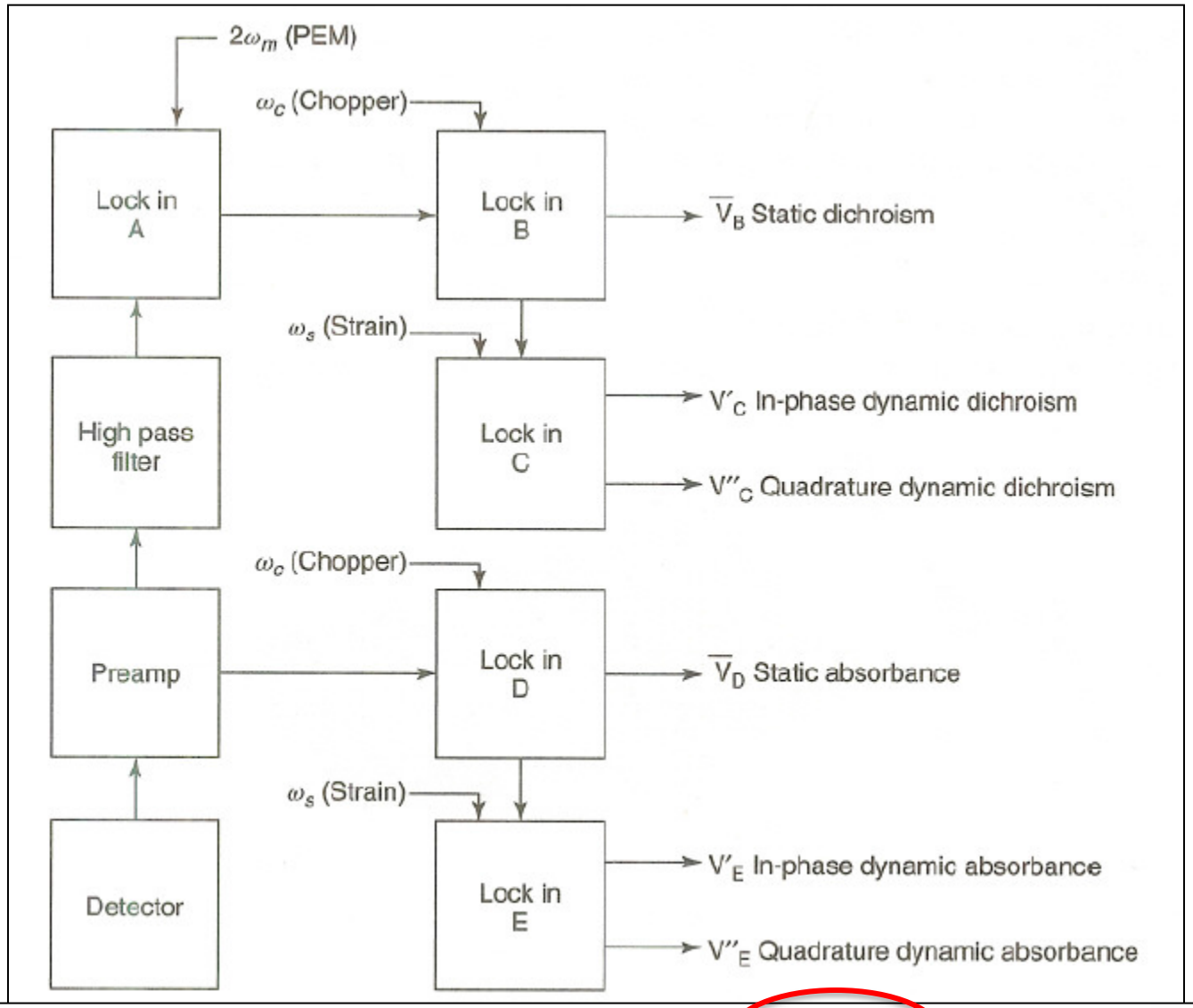

Figure 2. Configuration of the LIA train for the DIRLD spectrometer. [Reproduced from Noda *et al.*,[6] by permission of the Society for Applied Spectroscopy. © 1988.]

Layout (Diagram) Instrument

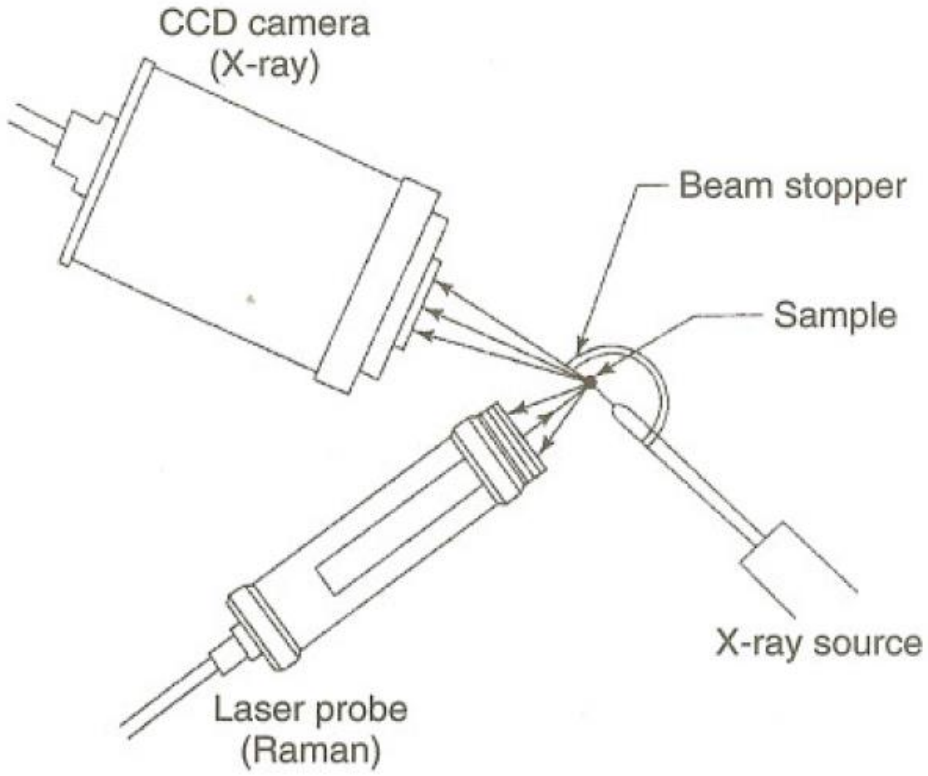

Figure 25. An illustration of the arrangement of the X-ray source, CCD camera and Raman laser probe around the sample for the simultaneous measurement of X-ray and Raman scattering.[68] [Reproduced from Kohji Tashiro, 'Measurement of the Physical Characteristics of Polymers', in "Handbook of Vibrational Spectroscopy", eds J.M. Chalmers and P.R. Griffiths, John Wiley & Sons, Chichester, 2437–2455, Vol. 4 (2002).]

Layout (Diagram) Instrument

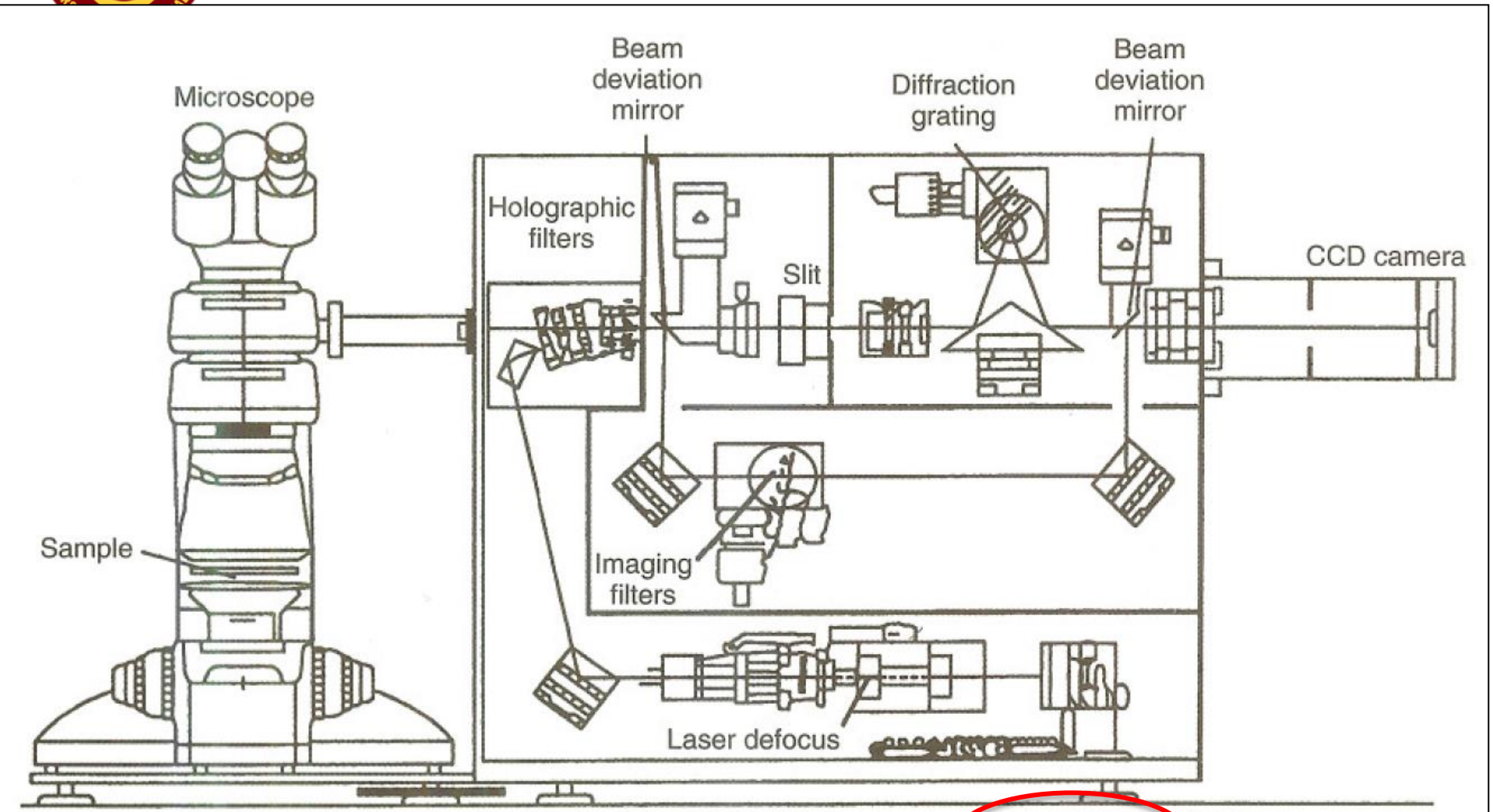

Figure 7. Schematic of a modern benchtop Raman microprobe spectrometer. [Diagram courtesy of Renishaw Pty. Ltd.]

Diagram

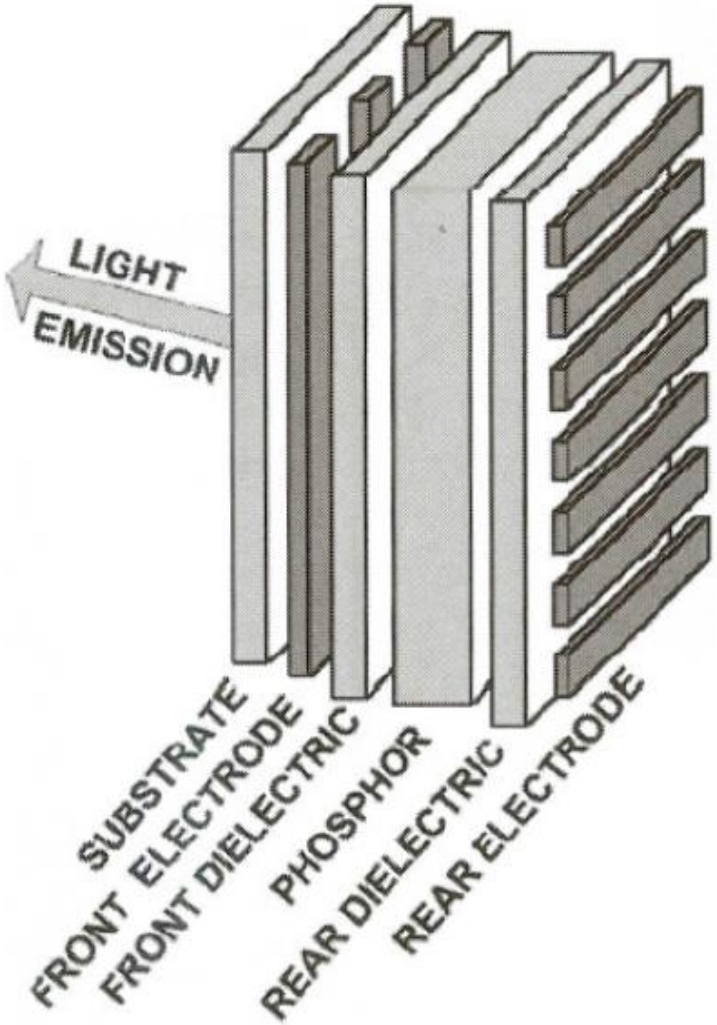

Figure 1a. Schematic diagram of a double-insulating TFEL device. A.N. Krasnov. Electroluminescent Displays: History and Lessons Learned. *Displays 24,* 73 (2003).

Diagram

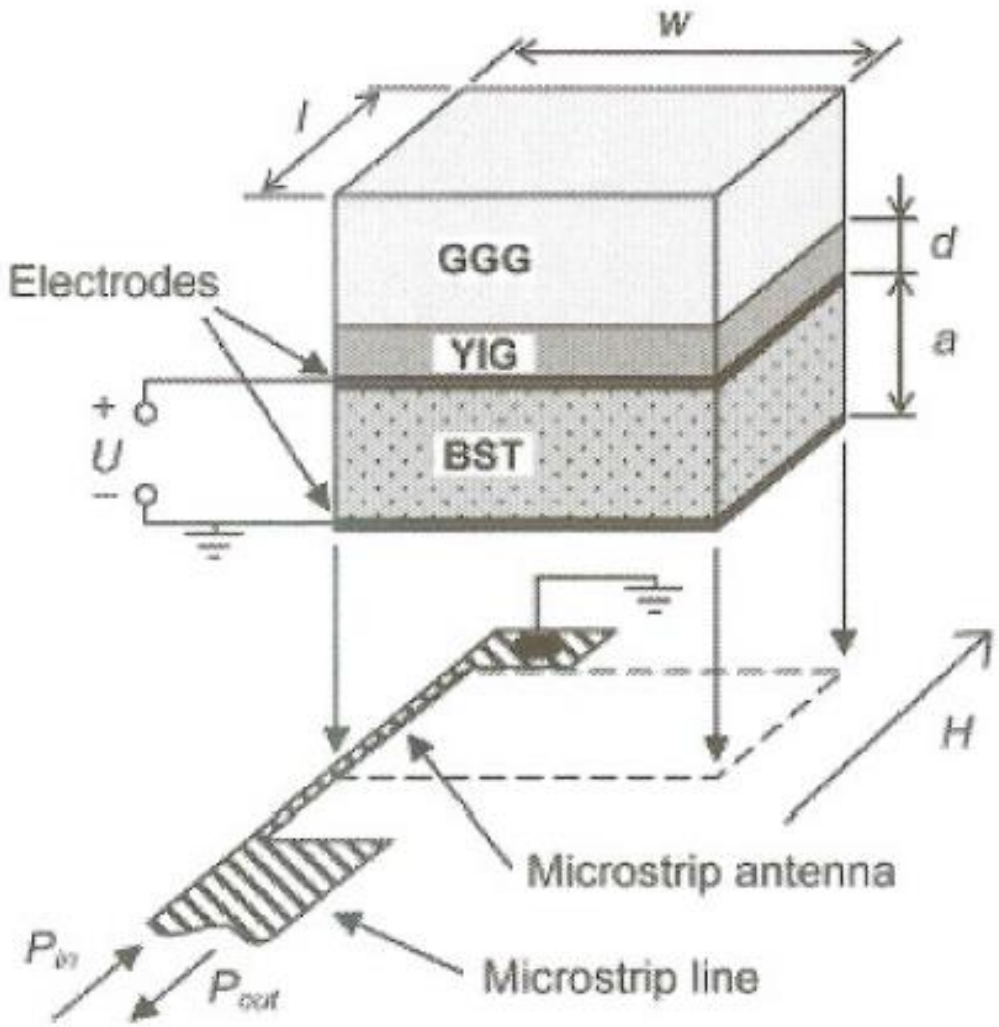

Figure 6.15 Diagram showing the schematics of a YIG–BST layered system for hybrid wave generation [50]. See also Color Insert.

Chemical Structure

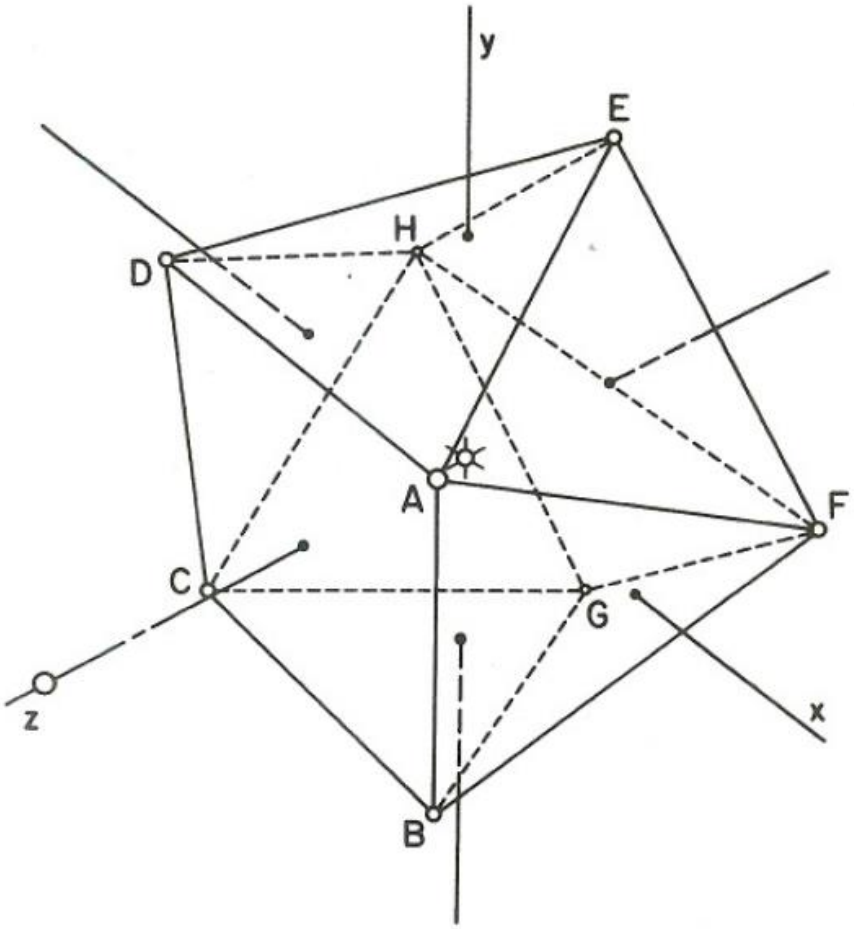

Fig. 16. Geometric model derived from field diagrams as those shown in Figure 15(b) and from some reasonable glass packing and density requirements. Result shown above is for an oxide such as the silicate glass. The Eu^{3+} sits at the center of this structure with a principal coordination of eight equidistant oxygens. A ninth oxygen (I) introduced along the z-axis distorts this structure by enlarging the *ABVD* area and by streching the *EFGH* plane towards negative z-values. From Brecher and Riseberg [99] and Weber [9].

Chemical Structure

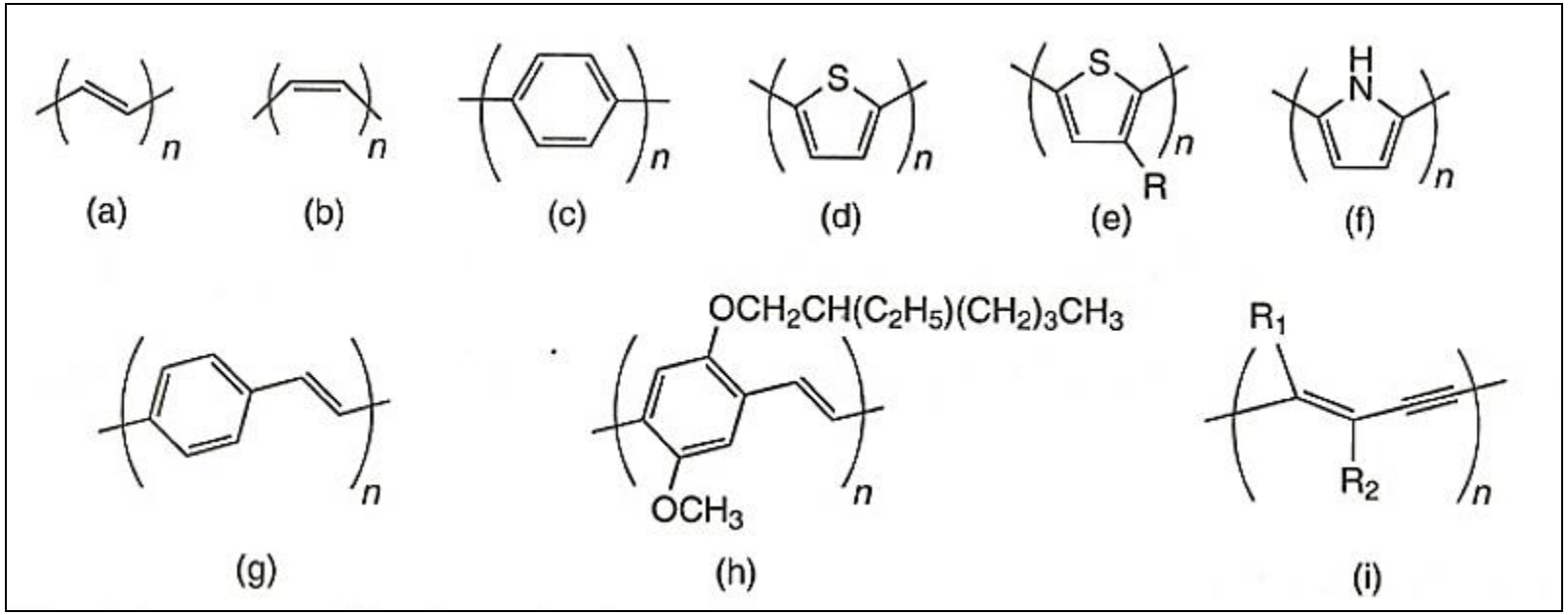

Figure 1. Chemical structures of conjugated polymers: (a) *trans*-polyacetylene; (b) *cis*-polyacetylene; (c) poly(*p*-phenylene); (d) polythiophenes; (e) regioregular poly(3-alkylthiophene); (f) polypyrrole; (g) poly(*p*-phenylenevinylene); (h) poly(2-methoxy-5-(2′-ethylhexyloxy)-*p*-phenylenevinylene) (MEH-PPV); (i) polydiacetylene. [Reproduced from Yukio Furukawa, 'Vibrational Spectroscopy of Conducting Polymers', in "Handbook of Vibrational Spectroscopy", eds J.M. Chalmers and P.R. Griffiths, John Wiley & Sons, Chichester, 2483–2495, Vol. 4 (2002).]

Photograph

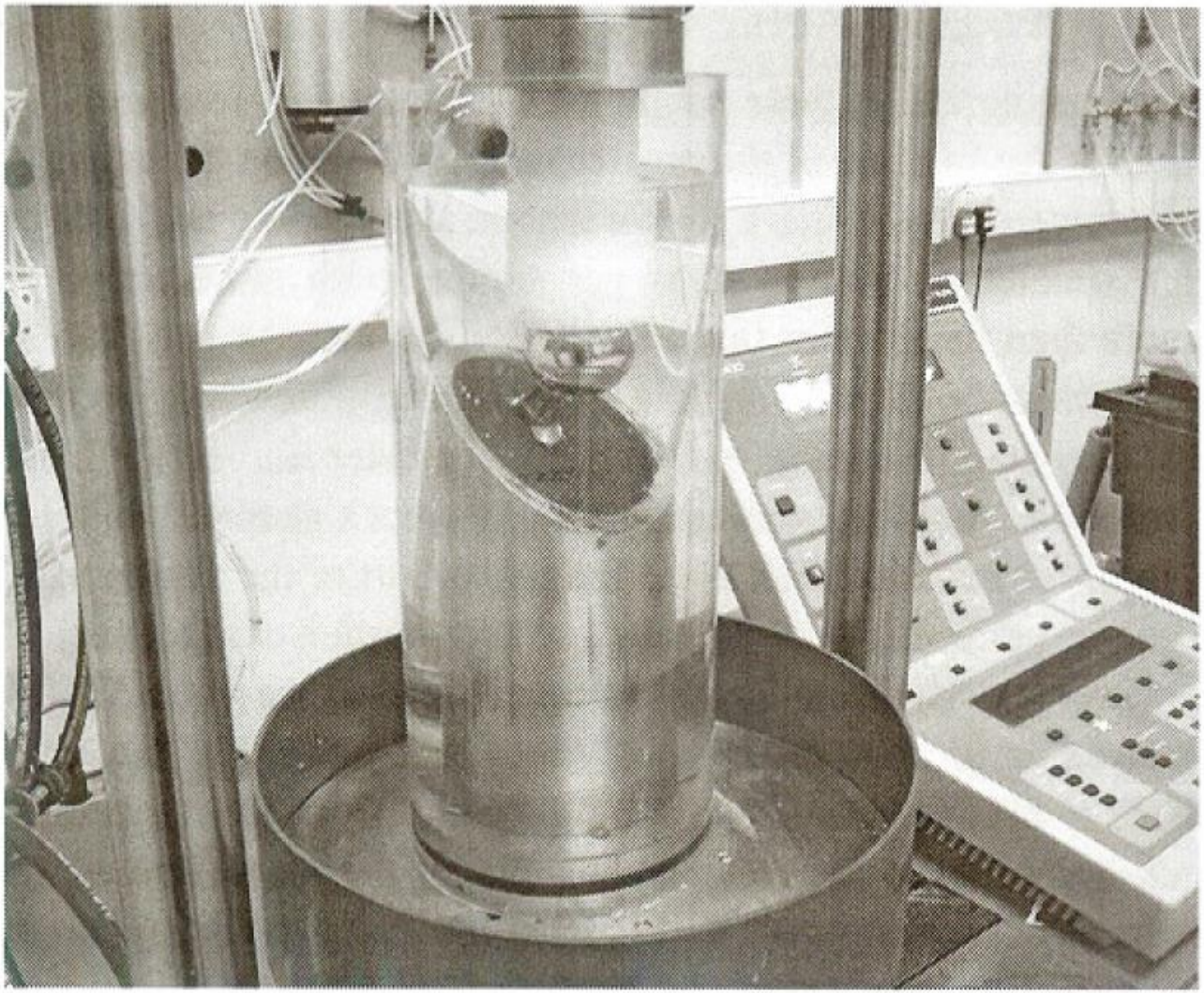

FIGURE 8.1 Femoral hip stem neck fatigue testing setup according to *ASTM F2068 – 09* [15]. (Image courtesy of Biomet).

Photograph

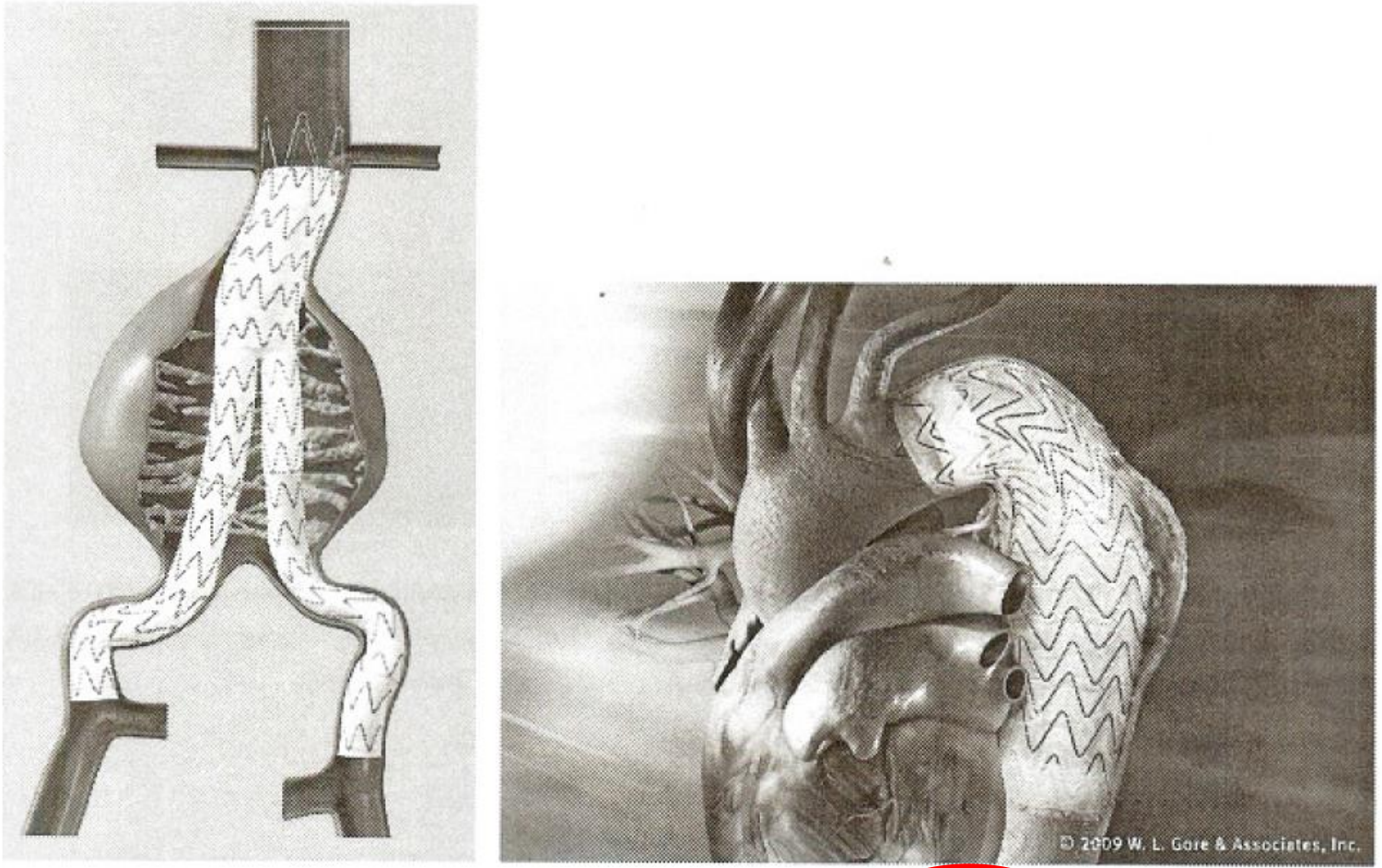

FIGURE 9.12 Endovascular stentgrafting in abdominal (left) *Source: Medtronic Inc. Reprinted with permission* and thoracic (right) aortic aneurysms. *Source: W.L. Gore & Associates, Inc. Reprinted with permission.*

Table

Table 1. Calculated depth resolution as a function of pinhole diameter and objective magnification.[39] Values in parentheses are experimentally determined. The 50×L objective is a long working distance objective.

	Pinhole diameter (μm)		
	500	300	100
Objective	Depth resolution (μm)		
50×	6.0 (7)	3.0 (6)	1.5 (3)
50×L	14	8.0	3.0
100×	3.0 (3)	1.5 (3)	0.7 (2)

Reproduced from R. Tabaksblat, R.J. Meier and B.J. Kip, *Appl. Spectrosc.*, **46**, 60 (1992) by permission of the Society for Applied Spectroscopy.

Graph

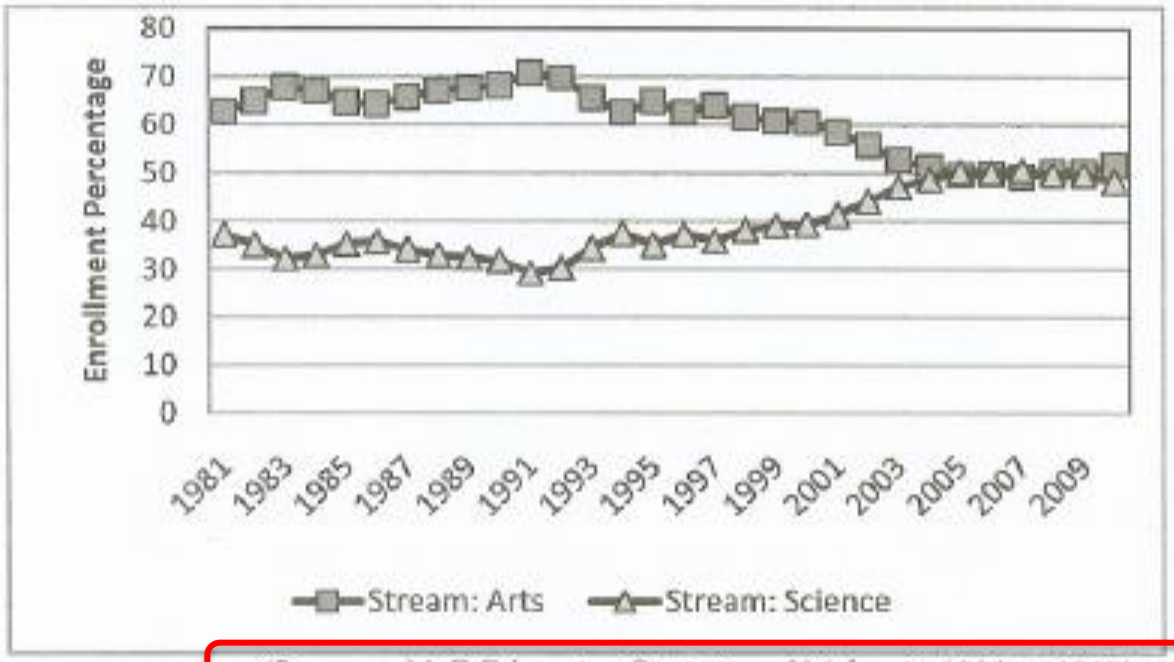

(Sources: MoE Education Statistics of Malaysia 1981 to 2010)

Graph 1 Percentage of enrollment of secondary school students in science (and technology) and art (and religion) streams (1981-2010)

Internet Source

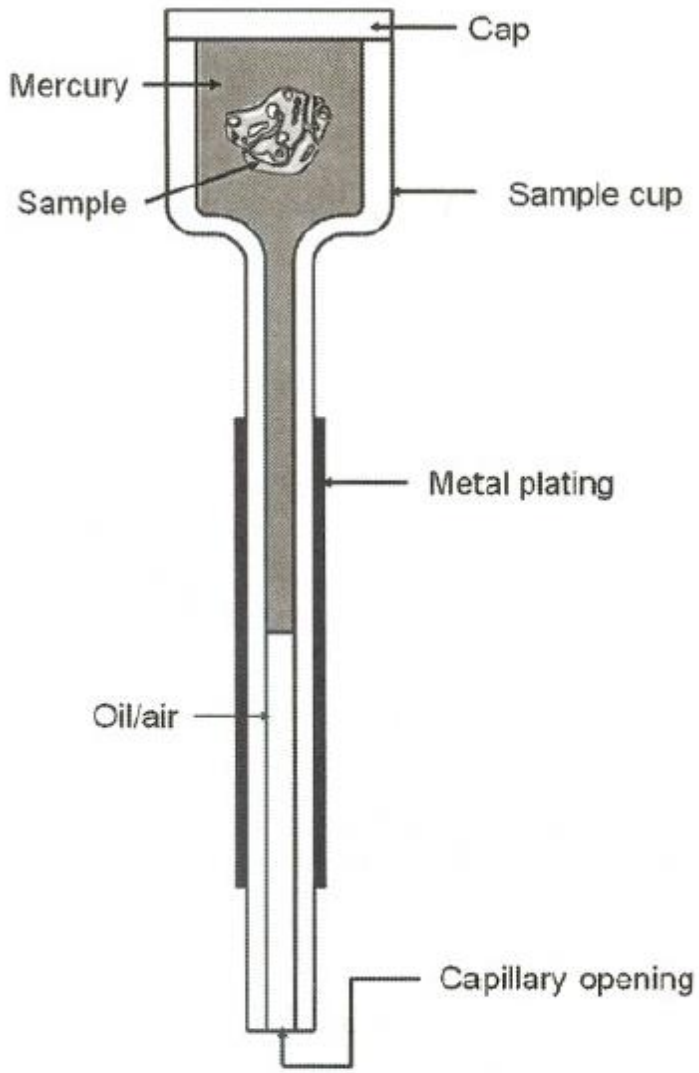

FIGURE 2.24 Cross-sectional view of a typical mercury penetrometer. *Source: Mercury Intrusion Porosimetry Theory, Presented by Micromeritics Instrument Corporation, www.micromeritics.com.*

Figure Journal

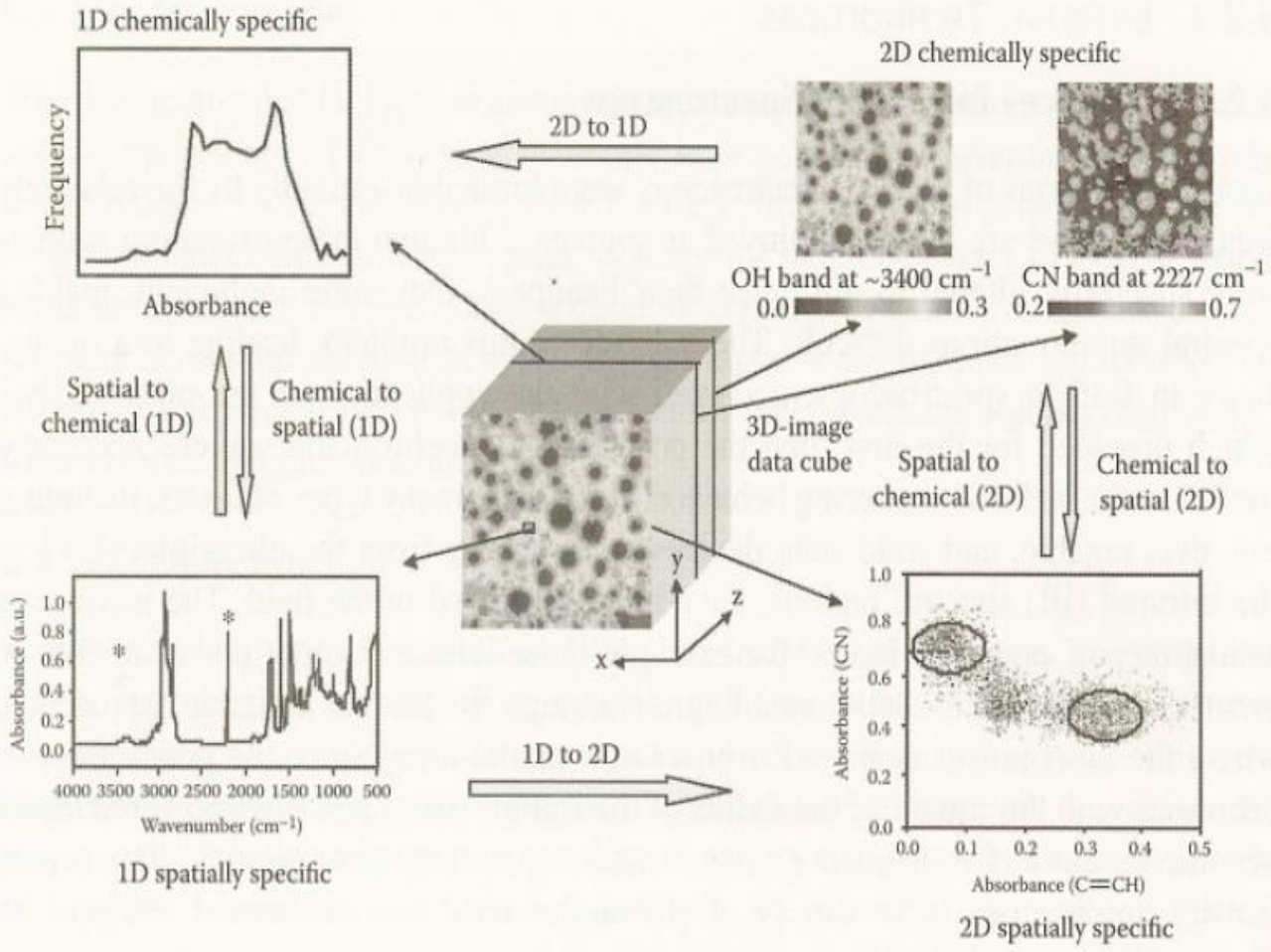

FIGURE 5.1 Visualizations afforded by an imaging data set. (Reproduced from R Bhargava, S-Q Wang, JL Koenig, *Adv. Polym. Sci.*, 163: 137, 2003)

Figure Journal

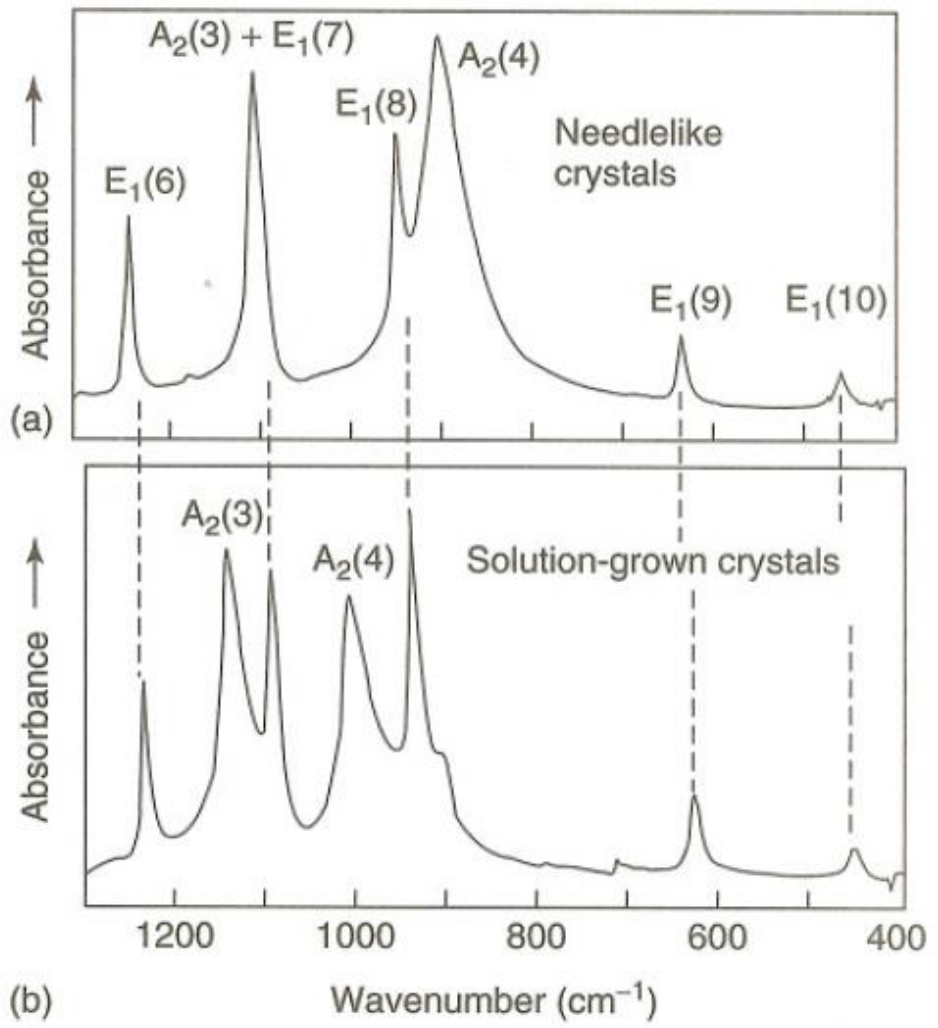

Figure 7. Infrared spectra of POM[34] (a) FCC and (b) FCC [Reproduced by permission of Kluwer Academic Publishers from M. Kobayashi, 283–294 in 'Crystallization of Polymers' M. Dosiere ed (1993).]

Figure Journal

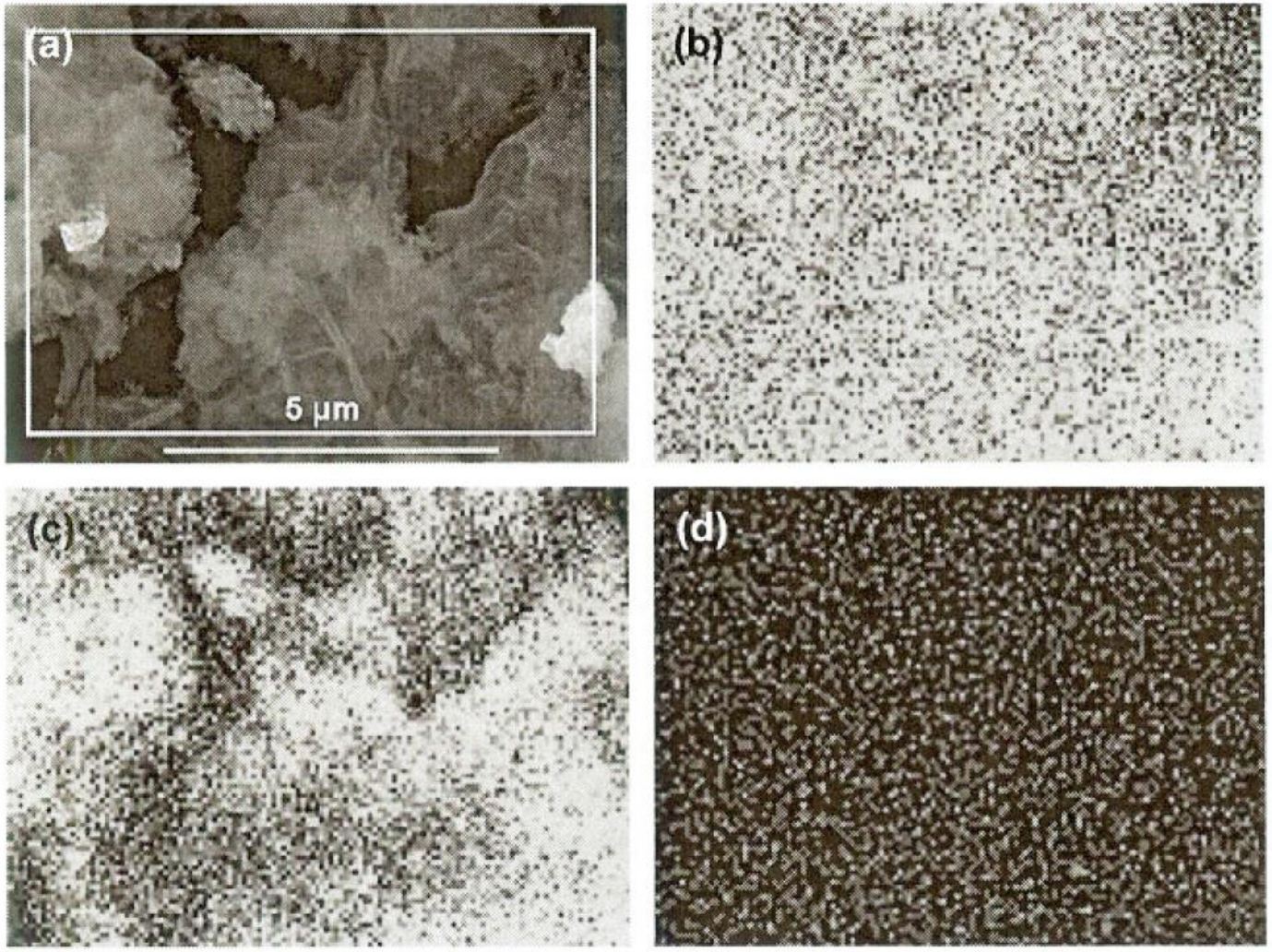

FIGURE 4.28 EDS elemental mapping: (a) Selected area on the sample (n-SrO-TiO_2 tubes); (b) Ti mapping; (c) O mapping; (d) Sr mapping. *Reprinted with permission from Ref. [150]. Copyright (2010) Elsevier.*

Unpublished Results

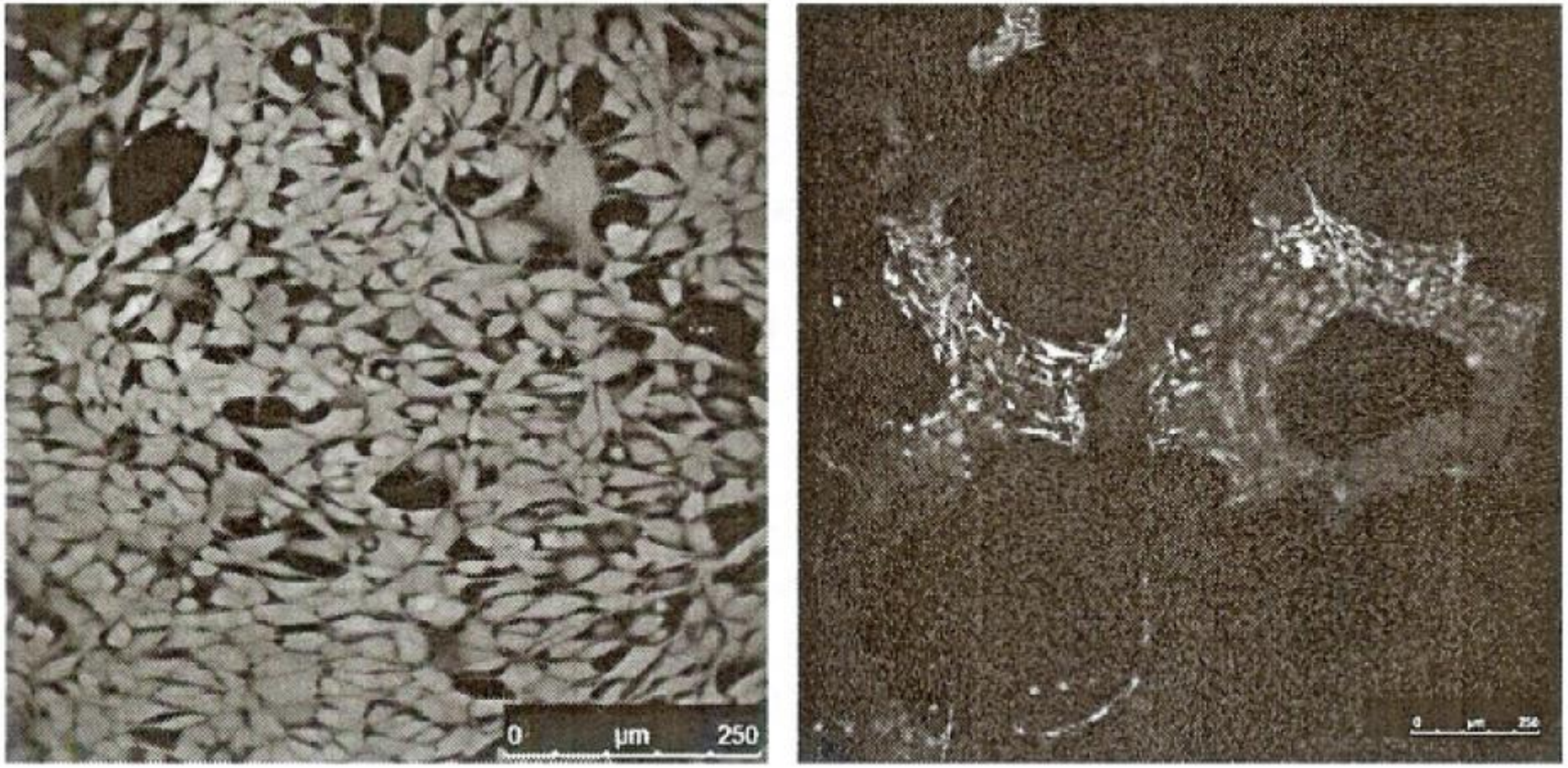

FIGURE 7.1.2 Fluorescence images of Live/Dead stained MG-63 osteoblast-like cells cultured on a dense disc (left) and on a three-dimensional bioactive glass scaffold (right). (Unpublished results, Institute of Biomaterials, University of Erlangen-Nuremberg).

Source: Thesis

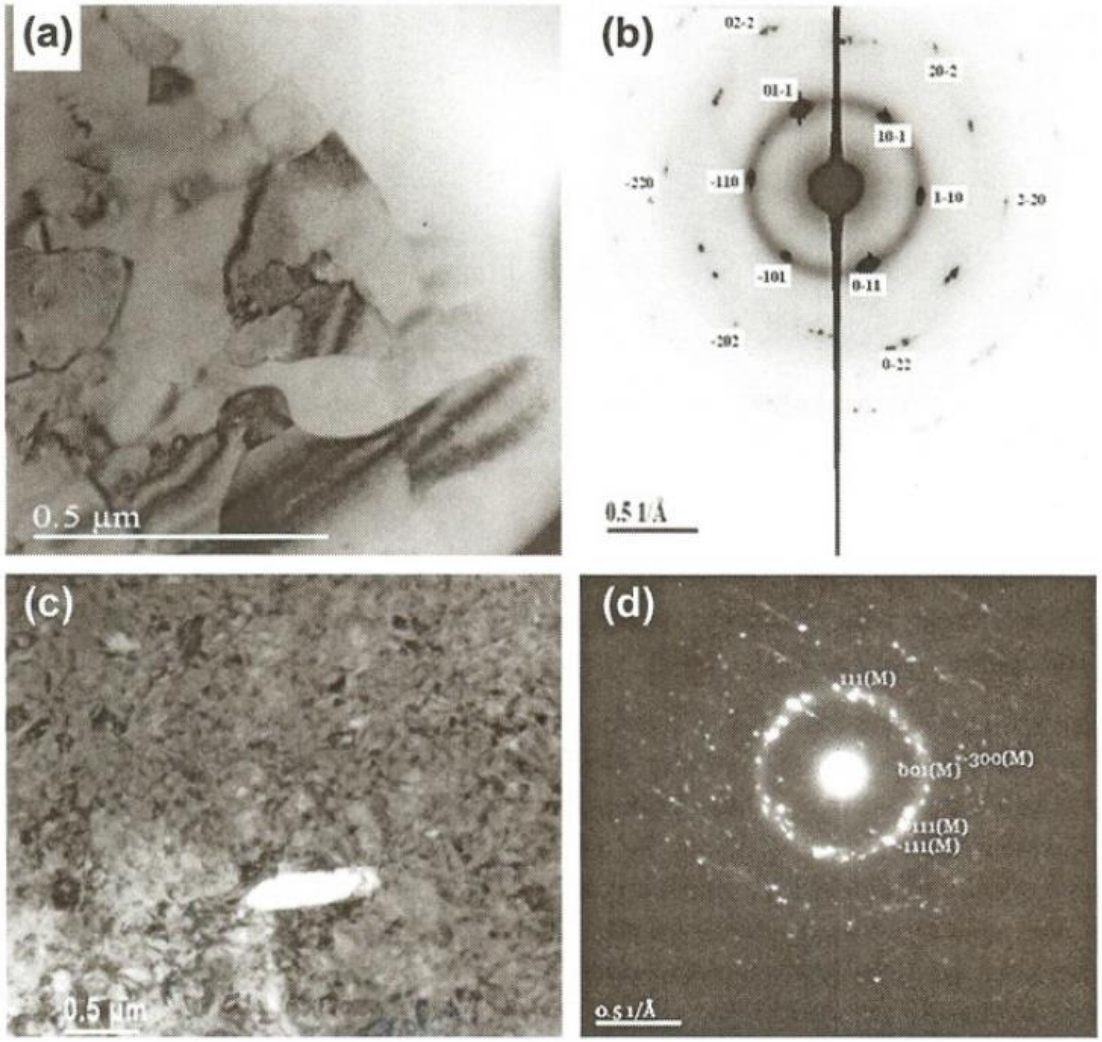

FIGURE 2.6 TEM micrograph and SAED pattern of austenite (a,b) and martensite (c,d) phases of NiTi alloy. *Source: Madhavi Tiyyagura, M.S. thesis, University of Central Florida, Orlando, Florida, 2005.*

Source Patent

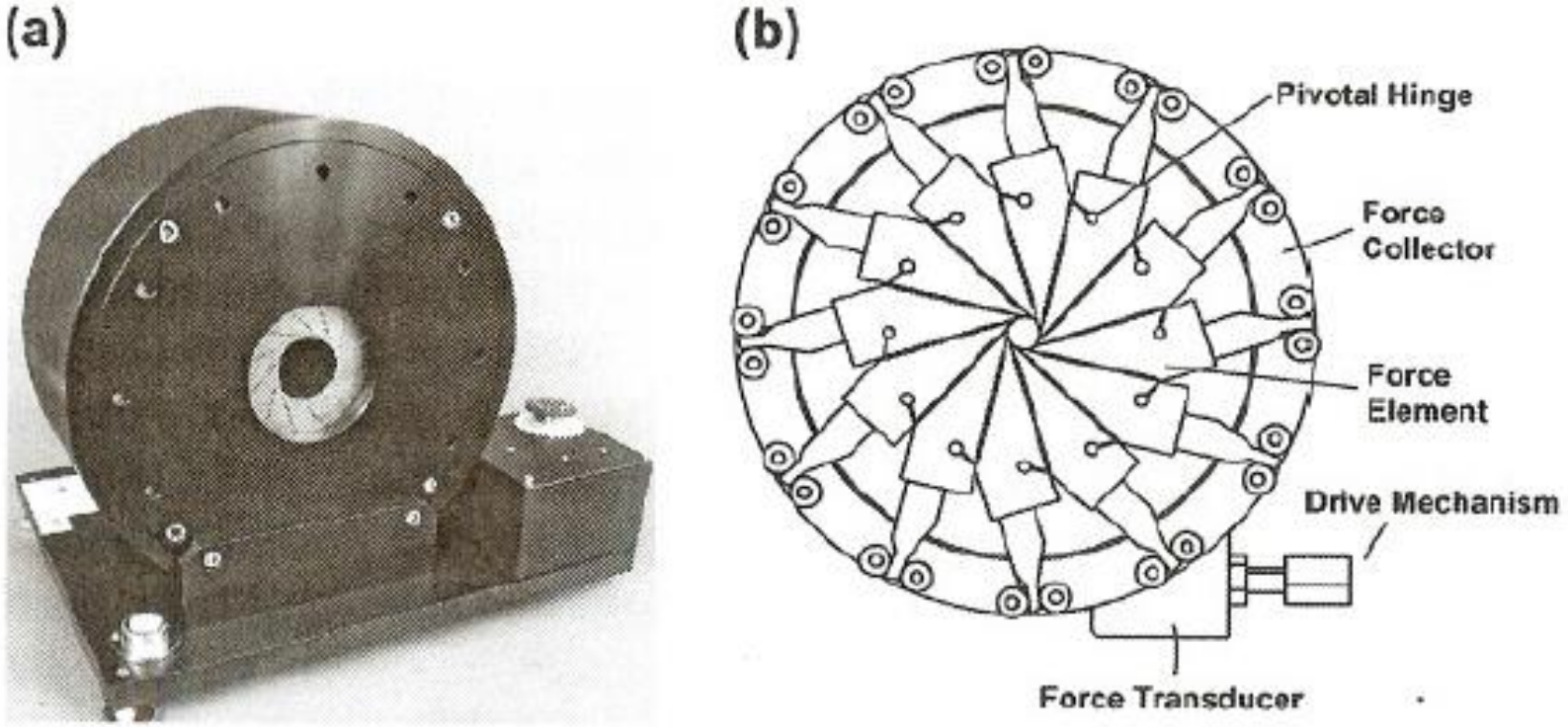

FIGURE 9.27 (a) Photograph and (b) construction of a segmented head radial force tester. *Source: United States Patent and Trademark Office; US7,069,794 B2.*